Cancer Gene Therapy (2013) 20, 17–24

www.nature.com/cgt

ORIGINAL ARTICLE

Combination of vinblastine and oncolytic herpes simplex virus vector expressing IL-12 therapy increases antitumor and antiangiogenic effects in prostate cancer models

BJ Passer[1], T Cheema[1], S Wu[2], C-I Wu[2], SD Rabkin[1] and RL Martuza[1]

Oncolytic herpes simplex virus (oHSV)-1-based vectors selectively replicate in tumor cells causing direct killing, that is, oncolysis, while sparing normal cells. The oHSVs are promising anticancer agents, but their efficacy, when used as single agents, leaves room for improvement. We hypothesized that combining the direct oncolytic and antiangiogenic activities of the interleukin (IL)-12-secreting NV1042 oHSV with microtubule disrupting agents (MDAs) would be an effective means to enhance antitumor efficacy. Vinblastine (VB) was identified among several MDAs screened, which displayed consistent and potent cytotoxic killing of both prostate cancer and endothelial cell lines. In matrigel tube-forming assays, VB was found to be highly effective at inhibiting tube formation of human umbilical vein endothelial cells. The combination of VB with NV1023 (the parental virus lacking IL-12) or NV1042 showed additive or synergistic activity against prostate cancer cell lines, and was not due to increased oHSV replication by VB. In athymic mice bearing CWR22 prostate tumors, VB in combination with NV1042 was superior to the combination of VB plus NV1023 in reducing tumor burden, appeared to be nontoxic and resulted in a statistically significant diminution in the number of $CD31^+$ cells as compared with other treatment groups. In human organotypic cultures using surgical samples from radical prostatectomies, both NV1023 and NV1042 were localized specifically to the epithelial cells of prostatic glands but not to the surrounding stroma. These data highlight the therapeutic advantage of combining the dual-acting antitumor and antiangiogenic activities of oHSVs and MDAs.

Cancer Gene Therapy (2013) **20,** 17–24; doi:10.1038/cgt.2012.75; published online 9 November 2012

Keywords: oncolytic HSV-1; prostate cancer; IL-12; angiogenesis; microtubule disrupting agents; combination therapy

INTRODUCTION

Selectively replication-competent viral vectors, such as oncolytic herpes simplex viruses (oHSVs) type 1 are genetically engineered from HSV type I. These lytic viruses represent an attractive strategy for tumor-based therapies, because they can specifically replicate and spread in cancer cells *in situ*, exhibiting oncolytic activity through direct cytopathic effects while sparing normal cells. Since the first report of a conditionally replicating genetically engineered virus,[1] a number of oHSV vectors have been developed, which are highly effective against a myriad of solid tumors.[2–5] For example, NV1023 and the interleukin (IL)-12-expressing NV1042 are derived from an HSV-1/2 intertypic mutant, which retains one copy of *gamma34.5* gene.[6] NV1042 has been shown to inhibit squamous cell carcinoma growth through both antiangiogenic mechanisms as well as direct cytopathic effects.[7] We have shown that NV1042 is superior to the NV1023 parent vector in inhibiting prostate cancer growth of both primary and metastatic tumors via both immune and antiangiogenic mechanisms in syngeneic mouse models.[8–10] The antiangiogenic activity is due, in part, to the induction of interferon-γ pro-inflammatory activities.[11] Interferon-γ affects the neovasculature through induction of the angiostatic chemokines CXCL9 (MIG) and CXCL10 (IP-10), upregulation of vascular cell adhesion molecule-1 and inhibition of matrix metalloproteinase 9 expression.[12] Although IL-12 is also known to enhance antitumor response by inducing a T-helper 1 response, it has also been shown that blood vessel formation is markedly decreased by IL-12 treatment in severe-combined immunodeficient mice,[11] suggesting that the antiangiogenic effects of IL-12 is independent of T and B cells.

Previously, we reported that the combination of oHSV plus a microtubule disrupting agent (MDA), that is, docetaxel or paclitaxel, acts synergistically to promote prostate cancer cell killing *in vitro* and *in vivo*.[13] Similar synergistic interactions have been reported for another HSV-1 mutant, as well as for vaccinia virus and reovirus in various cancers, including prostate cancer.[14–16] In addition, studies involving the use of adenovirus mutants in combination with either paclitaxel or docetaxel have reported synergistic interactions in prostate cancer cells.[17,18] MDAs have been shown to be effective inhibitors not only of tumor growth but also angiogenesis in numerous *in vivo* models.[19] To take additional advantage of a dual killing mechanism (tumor cells plus tumor endothelial cells) and to further improve upon the efficacy of currently available oncolytic vectors, we examined the strategy of using an 'armed' oHSV expressing IL-12 combined with an MDA. We have evaluated the preclinical therapeutic effects of NV1042 (expressing IL-12) in combination with vinblastine (VB) and showed that this combination enhances antitumor efficacy, in part, by inhibiting angiogenesis.

[1]Department of Neurosurgery, Brain Tumor Research Center, Massachusetts General Hospital and Harvard Medical School, Boston, MA, USA and [2]Department of Pathology, Massachusetts General Hospital and Harvard Medical School, Boston, MA, USA. Correspondence: Dr BJ Passer, Department of Neurosurgery, Brain Tumor Research Center, Massachusetts General Hospital and Harvard Medical School, Simches Research Building CRPZN 3800, 185 Cambridge Street, Boston, MA 02114, USA.
E-mail: bpasser@partners.org
Received 9 July 2012; revised 11 September 2012; accepted 11 September 2012; published online 9 November 2012

MATERIALS AND METHODS

Cells and viruses

Vero (African green monkey kidney), MS1 (mouse pancreatic endothelial), C166 (mouse yolk sac endothelial), CWR22 (human prostate cancer) and PC3 (human prostate cancer) cells were obtained from the American Type Culture Collection (Manassas, VA, USA) and human umbilical vein endothelial cells (HUVEC) were obtained from Lonza (Hopkinton, MA, USA). HBME-1 (human bone marrow endothelial) cells were a generous gift from Dr K Pienta (University of Michigan). Vero cells were grown in Dulbecco's modified Eagle's medium supplemented with 10% calf serum and HUVEC in EGM-2. PC3 cells were grown in FK-1 media containing 10% heat-inactivated fetal calf serum (Hyclone, Logan, UT, USA). Primary human prostate epithelial cells and its culture medium PrEGM were maintained as described by the manufacturer (Lonza). Construction of NV1023 and NV1042 has previously been described.[20] NV1023, derived from NV1020 (R7020), a HSV-1/2 intertypic recombinant developed as a vaccine strain,[21] contains an insertion of *LacZ* into the *ICP47* locus, deleting *ICP47*, *US11* and *US10*.[20] NV1042 is NV1023 with an insertion of murine IL-12 cDNA (p35 and p40 as a single polypeptide separated by elastin motifs) expressed from a hybrid α4-TK promoter.[20]

Cell viability assays

Viability assays were performed over a 3-day period using the MTS (3-(4,5-dimethylthiazol-2-yl)-5-(3-carboxymethoxyphenyl)-2-(4-sulfophenyl)-2H-tetrazolium) assay kit (Promega, Madison, WI, USA) in a 96-well format. The compounds used in this study included, Paclitaxel (Bristol-Myers Squibb, Princeton, NJ, USA), docetaxel (Aventis Pharmaceuticals, Bridgewater, NJ, USA), VB (APP Pharmaceuticals, Schaumburg, IL, USA), epothilone-B (Sigma-Aldrich, St Louis, MO), vincristine (Hospira, Lake Forest, IL, USA) and 2-methoxyestradiol (Sigma-Aldrich).

Virus titration

Monolayer cultures of Vero cells grown in a six-well plate were infected with serial dilutions of virus. After removal of virus inoculum, the cells were incubated in Dulbecco's modified Eagle's medium supplemented with 1% inactivated fetal calf serum and 0.1% pooled human immunoglobulin at 37 °C for 3–4 days until plaques were visible and counted.

Virus replication assay

Cells were seeded in 12-well plate 1 day before infection and infected with NV1023 or NV1042 at a multiplicity of infection (MOI) of 1. At the times indicated, cells were collected from the wells and viral titers were determined on Vero cells. Prostate cancer and endothelial cell lines either remained untreated or were pretreated with VB (0.1 nM) for 12 h and, thereafter, cells were infected with NV1023 or NV1042 at an MOI of 1.5. At 24 or 48 h after infection, cells were scraped into the medium and subjected to three freeze–thaw cycles. Virus titers were determined by plaque assays on Vero cells. Each concentration in an experiment was plated in duplicate, and each experiment was performed three times. Supernatants collected from single burst assays were assayed for IL-12 derived from NV1042 at the indicated time points by enzyme-linked immunosorbent assay (R&D Systems, Minneapolis, MN, USA) and normal goat IgG (2 μg ml^{-1} per well; R&D Systems) was included as a species-specific control.

Cell susceptibility assays and Chou–Talalay analysis

Prostate cancer (PC3 and CWr22) and endothelial (HUVEC, HBM-1, C166 and MS1) cells were seeded into 96-well plates at 1500–3000 cells per well. Viability assays will be performed over a 3-day period using the MTS assay kit (Promega), with a concentration range of MDAs and varying MOIs of oHSV. Dose–response curves were generated using GraphPad v5.0 (GraphPad Software, San Diego, CA, USA). For Chou–Talalay analysis, dose–response curves and 50% effective dose values were obtained and compared at day 3. For 50% effective dose value determination, cells were incubated for 3 days with varying concentrations or MOIs of drug and virus, respectively, and cell survival was then assessed using MTS assays. Dose–response curves were fit to Chou–Talalay lines, which are derived from the law of mass action and are described by the equation $\log(f_a/f_u) = m \log D - m \log D_m$, in which f_a is the fraction affected (percent cell death), f_u is the fraction unaffected (percent cell survival), D is the dose, D_m is the median-effect dose (the dose causing 50% of cells to be affected, that is, 50% survival) and m is the coefficient signifying the shape of the dose–response curve. The combination index (CI)-isobologram by Chou and Talalay[22] was used to analyze virus and drug combinations. Fixed ratios of virus and drug concentrations, and mutually exclusive equations were used to determine CIs. All experiments were repeated at least three times.

Tube formation assay

HUVEC cells (~90 000 cells per well) were added to Matrigel (BD Biosciences, San Jose, CA, USA)-coated 24-well plates. Four hours later, docetaxel (10 nM), VB (10 nM), vincristine (10 nM), epothilone-B (10 μM) or 2-methoxyestradiol (10 μM) were added in triplicate. For combination studies, NV1023 or NV1042 (MOI 1) with or without VB (1 nM) were added. Twenty hours later, tube formation was quantified by counting the branching points for each well by light microscopy.

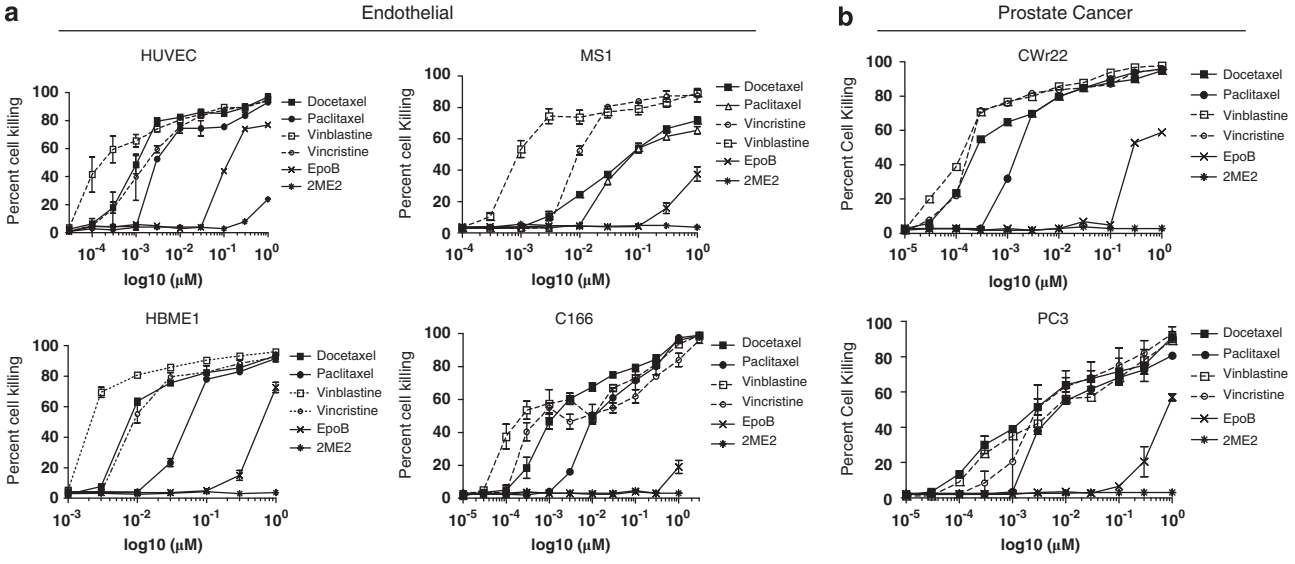

Figure 1. Cytotoxic effects of microtubule disrupting agents (MDAs). (**a**) HUVEC (human umbilical vein endothelial cells) primary cultures and endothelial cell lines MS1 (mouse pancreatic), C166 (mouse yolk sac), HBME-1 (human bone marrow) and (**b**) human CWR22 and PC3 prostate cancer cell lines were treated with increasing concentrations of the indicated MDAs. MTS (3-(4,5-dimethylthiazol-2-yl)-5-(3-carboxymethoxyphenyl)-2-(4-sulfophenyl)-2H-tetrazolium) assays were performed on day 3 to determine the extent of cell killing.

Table 1. Cytotoxicity of MDA's in human prostate cancer and endothelial cell lines

	Doc	*Pac*	*VB*	*VC*	*epoB*	*2ME2*
PCa endothelial						
HUVEC	0.88 ± 0.2	2.5 ± 1	0.18 + 0.04	1.7 ± 0.3	540 ± 56	>1000
HBME-1	7.8 + 2	53 ± 12	1.7 + 0.5	8.6 ± 2	540 ± 45	>1000
MS1	82 ± 11	98 ± 14	1.6 + 0.4	8.2 ± 3	>1000	>1000
C166	1.9 ± 0.1	12 ± 4	0.38 + 0.1	0.64 ± 0.1	>1000	>1000
CWR22	0.28 ± 0.3	1.7 ± 0.7	0.27 ± .02	0.26 ± .03	290 ± 35	>1000
Pc3	4.6 + 0.8	6.1 ± 1	7.8 ± 1	6.3 ± 0.5	890 ± 76	>1000

Abbreviations: 2ME2, 2-methoxyestradiol; Doc, docetaxel; epoB, epothilone-B; HBME-1, human bone marrow endothelial 1; HUVEC, human umbilical vein endothelial cell; MS1, mouse pancreatic endothelial; Pac, paclitaxel; VB, vinblastine; VC, vincristine.
Values represent EC_{50}; mean (nM) ± s.e.m.; 3-day.

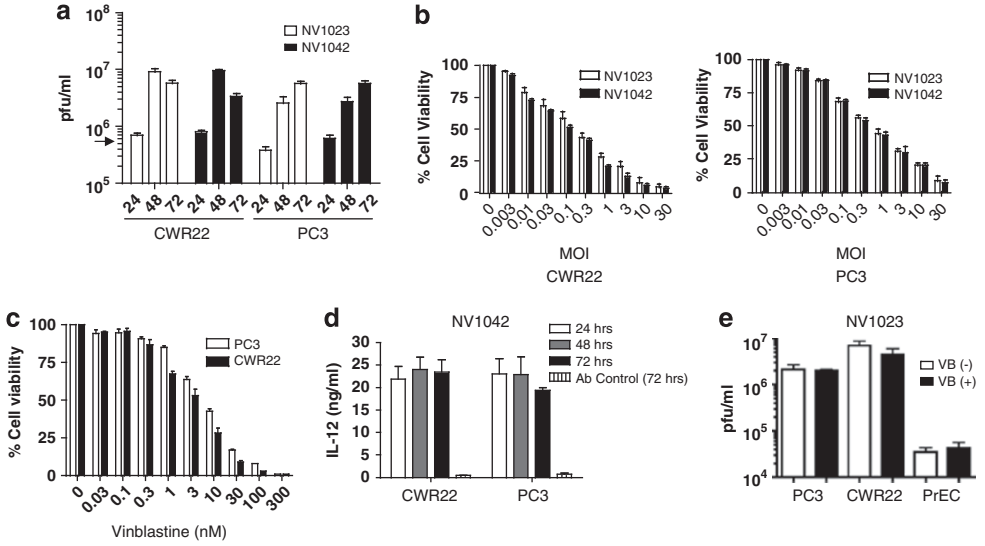

Figure 2. Analysis of NV1023 and NV1042 replication and effects on prostate cancer cell killing (**a**) Single burst assays were performed using either NV1023 or NV1042 (multiplicity of infection (MOI) = 1.5) on CWR22 or PC3 cells over a 72-h period. Virus (cell pellet plus supernatants) on days 1, 2 and 3 post infection and viral titers (pfu ml^{-1}) determined by plaque assay on Vero cells as described previously.[13] Input virus: $\sim 4 \times 10^5$ plaque-forming units (pfu; indicated by arrow). (**b**) Cell susceptibility assays were performed using NV1023 or NV1042 on either CWR22 (left) or PC3 (right) prostate cancer cells. Cell lines were inoculated with the indicated MOIs of virus, and cell killing was evaluated by MTS (3-(4,5-dimethylthiazol-2-yl)-5-(3-carboxymethoxyphenyl)-2-(4-sulfophenyl)-2H-tetrazolium) assay on day 3 (error bars represent s.e.m.). (**c**) PC3 (open bar) or CWR22 (solid bar) prostate cancer cells were treated with increasing concentration of vinblastine (VB; 0.01–100 nM) and MTS assays were performed to generate dose–response curves. (**d**) Supernatants collected from single burst assays were assayed for interleukin (IL)-12 derived from NV1042 by enzyme-linked immunosorbent assay at the indicated time points. NV1023 was used as a control vector to normalize for background and normal goat IgG control was also included to demonstrate specificity for murine IL-12. (**e**) Prostate cancer (PC3 and CWR22) and normal prostate epithelial (PrEC) cells were incubated in the presence or absence of nontoxic concentrations of VB (0.1 nM) for 12 h and, thereafter, cells were infected with NV1023 (MOI of 1.5) for 72 h. Virus titers were determined by plaque assay on Vero cells. Note that virus replication is not altered in the presence of VB and is negligible in PrEC.

In vivo studies

CWr22 cells (5×10^6 cells) were implanted subcutaneously into the flanks of 6- to 8-week-old balb/c *nu/nu* mice ($n = 8$ mice per group). When the tumor volume reached 75–150 mm^3 (~14 days after implantation), mice were stratified by tumor volume and then randomly assigned to treatment groups ($n = 8$ per group). Virus (NV1023 or NV1042; 5×10^5 plaque-forming units (pfu)) or virus suspension buffer (phosphate-buffered saline with 10% glycerol) was injected intratumorally on days 13 and 15 after tumor implantation. VB monotherapy or its combination with virus was administered intraperitoneally on day 15 at 0.35 mg kg^{-1} for 9 consecutive days. All procedures were approved by the MGH Subcommittee on Research Animal Care. Tumor volume was calculated using the formula width $(mm)^2 \times$ length (mm) $\times$ 0.52.

CD31 immunohistochemistry and quantification

Mice ($n = 3$ per group) were treated as described above, and at day 30 post-implantation tumors were collected, frozen and cut into tissues sections. Tissue sections were stained with a rat anti-mouse CD31 antibody (BD Biosciences), followed by secondary anti-rat IgG conjugated to horseradish peroxidase (GE Healthcare, Piscataway, NJ, USA). $CD31^+$ staining was revealed with 3,3′-diaminobenzidine histochemistry (Vector Laboratories, Burlingame, CA, USA). Sections were counterstained with hematoxylin (Sigma, St Louis, MO, USA). Tumor microvessel density was quantified for all treatment groups. At least 6–10 representative $\times$ 40 fields per view were captured as epifluorescent digital images using a Spot digital camera (Spot Diagnostic Instruments, Sterling, MI, USA). To calculate microvessel density, area occupied by CD31-positive microvessels and total tissue area, per section were quantified using Image J software (NIH, Bethesda, MD, USA). Microvessel density was then calculated as a percentage of CD31 stained per tumor section.

Prostate organ cultures

Prostate organ cultures were performed as previously described.[23] Briefly, tissue fragments were incubated with NV1023 (1×10^6 pfu) or NV1042 (1×10^6 pfu) for 1 h in direct contact and, thereafter, placed on a

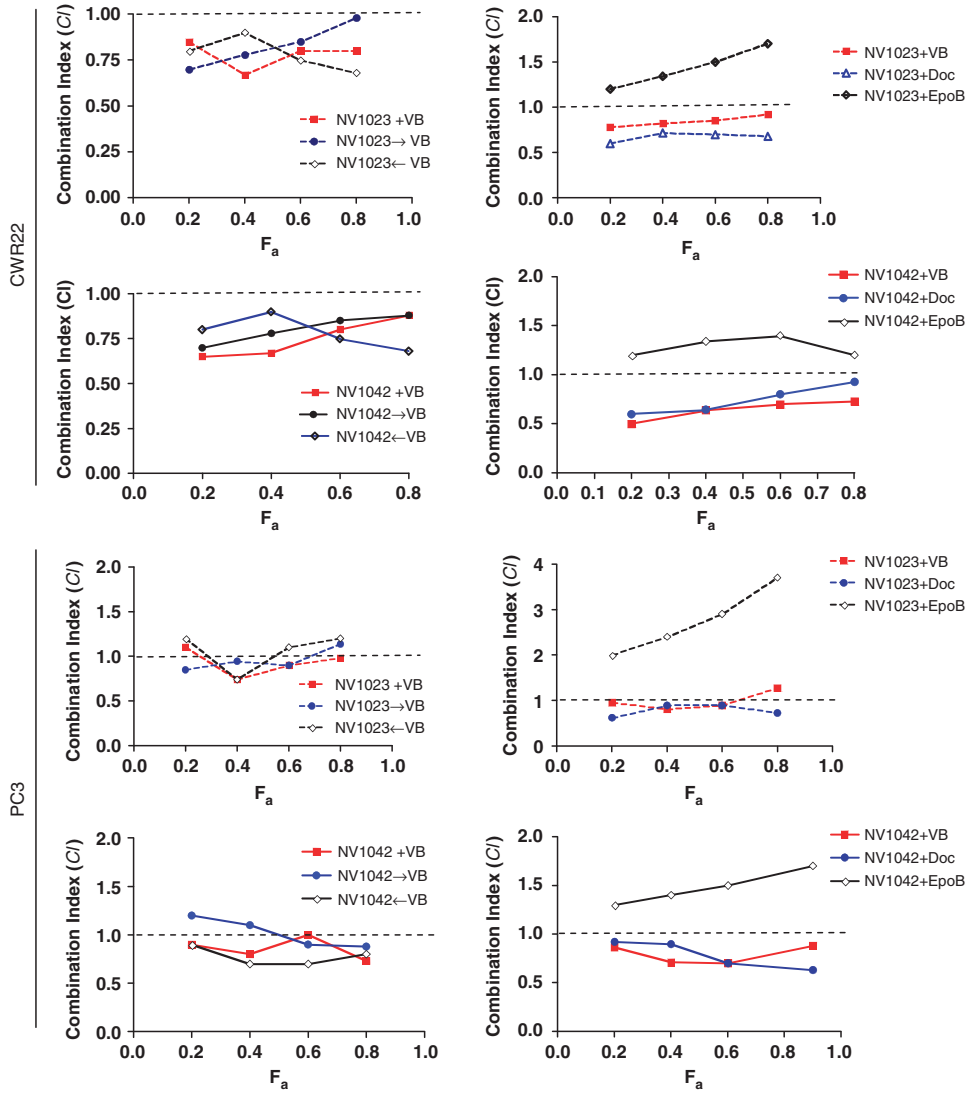

Figure 3. Combination index (CI) analysis. Fraction affected (F_a) versus CI plots were generated using the method of Chou and Talalay[22] to determine the extent of synergy if any for either vinblastine (VB), docetaxel (Doc) or epothilone-B (EpoB) in combination with NV1023 or NV1042 in CWR22 (upper panels) and PC3 (lower panels) cell lines. + Simultaneous oncolytic herpes simplex virus (oHSV) and drug addition; → oHSV inoculation 24 h before drug treatment; ← drug treatment 24 h before oHSV infection. Synergistic effects are defined as CI < 1 additive effects are CI = 1, and antagonistic effects are CI > 1. Note that the dotted line in each plot indicates a reference point of a CI value of 1.

semi-submersed collagen sponge (Ultrafoam, Davol, Warwick, RI, USA) for 3 days. Tissue specimens (8 μm) were stained with anti-HSV-1 gC (Virusys, Sykesville, MD, USA) or anti-cytokeratin-8/18 (UCD/PR-10.11; Dako-cytomation, Carpinteria, CA, USA) antibodies as previously described. Virus titers were determined by titration of tissue homogenates on Vero cells using plaque assays. Tissues weights were determined to correct for viral titer concentrations (average ± s.e.m.). Each color dot indicates a different prostate surgical specimen that was separately infected with either NV1023 or NV1042 ($n = 5$).

Statistical analysis

All statistical analyses were done using GraphPad prism v5. For comparison of efficacy and mechanism of efficacy, unpaired Student's *t*-test (two-tailed) was used to analyze significance between two treatment groups.

RESULTS

Evaluation of a panel of MDAs on endothelial and prostate cancer cell lines

MDAs have been shown to have broad-based antitumor and antiangiogenic properties.[19,24] We initially screened a series of MDAs (docetaxel, paclitaxel, VB, vincristine, epoB and methoxyestradiol) on a panel of human- (HUVEC, HBME-1) and mouse-derived (MS1 and C166) endothelial and human prostate cancer cell lines. Although the majority of MDAs tested yielded potent cytotoxic effects on all four endothelial cell lines, VB was consistently superior ($EC_{50} = 0.18–1.7$ nM), demonstrating a potent dose-dependent endothelial cell killing (Figure 1a and Table 1). *In vitro* matrigel assays, which partially recapitulate the mechanisms of neovascularizaion observed *in vivo*, confirmed that VB was highly effective at inhibiting tube formation of HUVEC cells (Supplementary Figure 1). Furthermore, in prostate cancer cell lines, VB was more or equally potent as the other MDAs tested. For example, in the androgen-dependent CWR22 cell line, the cytotoxic effects of VB paralleled vincristine, whereas VB's cytotoxic effects on the androgen-independent PC3 cell line was similar to vincristine, docetaxel and paclitaxel (Figure 1b and Table 1). In contrast, epothilone-B and 2-methoxyestradiol had negligible effects on both endothelial and tumor cell lines. Lastly, when endothelial (HUVEC and HBME) or prostate cancer cells (CWR22 and PC3) were treated with MDAs for only 3 h and then

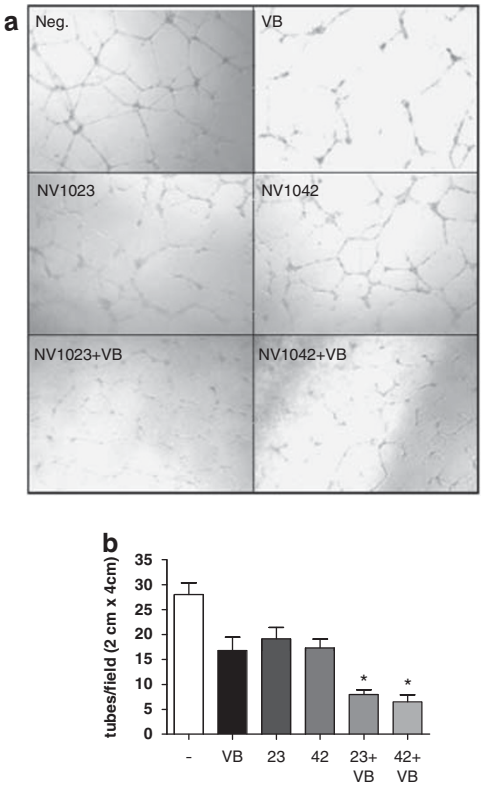

Figure 4. Increased antiangiogenic effects of NV1042/vinblastine (VB) combination in an *in vitro* tube formation assay. HUVEC cells (human umbilical vein endothelial cells) were plated on matrigel-coated plates and either remained untreated (negative (Neg.)) or treated with NV1023 or NV1042 (multiplicity of infection (MOI) 1), VB (1 nM) or their combination. Twenty hours later, tube formation was scored. Representative fields are shown for each condition (**a**) and the number of tubes/field was quantified (**b**). Each treatment was performed in triplicate. Student's *t*-test was used to determine statistical significance between the indicated control and treatment groups. Bars represent average ± s.e.m. $*P<0.01$ for NV1023 + VB and NV1042 + VB versus NV1023 alone, NV1042 alone, VB alone or untreated.

washed away, VB was still cytotoxic, suggesting that even transient exposure of VB is effective (Supplementary Figure 2).

In vitro assessment of oHSV and MDA combination

Previously, we reported that NV1023 and IL-12-secreting NV1042 were effective *in vitro* and *in vivo* at killing mouse prostate cancer cells.[8–10] To evaluate the cellular permissiveness of the human CWR22 and PC3 cancer cell lines toward NV1023 and NV1042, we performed viral burst assays. Figure 2a shows that by 48 h, virus production in CWR22 cells peaked, resulting in an ~32-fold increase in viral titers over input virus. By 72 h, the generation of virus progeny had plateaued. In PC3 cells, NV1023 and NV1042 virus production steadily increased over a 72-h time period, resulting in a ~22-fold enhancement over input virus. Dose–response curves reflected the above findings, with both NV1023 and NV1042 more cytopathic toward CWR22 ($EC_{50}=0.24$; MOI) than PC3 ($EC_{50}=0.85$ MOI) cells (Figure 2b). In addition, VB treatment of PC3 ($EC_{50}=7.8$ nM) and CWR22 ($EC_{50}=4.2$ nM) resulted in a dose-dependent response over a 3-day period (Figure 2c). IL-12 secretion after NV1042 infection showed relatively high levels in both prostate cancer cell lines over a 72-h period, even though differences in viral titers were observed between cell lines (Figure 2d). Lastly, both NV1023 and NV1042 (data not shown) can replicate to various degrees in the four aforementioned endothelial cell lines (Supplementary Figure 3).

We used the CI method of Chou and Talalay[22] to assess whether the parental virus NV1023 in conjunction with VB could promote CWR22 or PC3 cell killing in a synergistic manner. A CI value of less than1 indicates synergism and CI > 1 indicates antagonism. Mild synergism (CI ~ 0.8) was observed when NV1023 or NV1042 ($EC_{50}=0.24$ MOI) and VB ($EC_{50}=4.2$ nM) were added together in CWR22 cells (Figure 3). We further explored whether the observed synergistic effect was dependent on the timing of drug administration. A similar synergistic effect (CI ~ 0.8) was observed regardless of whether VB was added 12 h before or after treatment of NV1023 or NV1042 (Figure 3c). Lastly, docetaxel but not epothilone-B could be substituted for VB in combination with NV1023 or NV1042, resulting in mild synergy (Figure 3c). In PC3 cells, the combination of NV1023 or NV1042 ($EC_{50}=0.85$ MOI) with VB ($EC_{50}=7.8$ nM) resulted in an additive effect regardless of the order of administration. We also addressed whether the observed synergistic effects were due to increased oHSV replication by VB. The addition of a nontoxic concentration of VB (0.1 nM) to NV1023 neither increased nor decreased viral titers as compared with NV1023 alone at 48 h after infection in single-step growth curve assays (Figure 2e). Lastly, in matrigel tube formation assays, we observed that the combination of either NV1023 or NV1042 (MOI 0.2) with VB (1 nM) was significantly more effective at disrupting tube formation than any single agent alone (Figure 4).

Preclinical evaluation NV1023 or NV1042 with VB in CWR22 xenografts

Next, we evaluated the *in vivo* antitumor efficacy of NV1023 or NV1042 in combination with VB in subcutaneous CWR22 tumors in athymic mice. Initially, doses of individual therapies were established to determine conditions resulting in tumor size reductions of 20–50% (data not shown). Mice were treated with either mock control, NV1023 or NV1042 (5×10^5 pfu) on days 13 and 15, and/or VB (0.35 mg kg^{-1}; for 9 consecutive days) starting on day 15 (Figure 5a). By 32 days after tumor implantation, a statistically significant decrease in tumor volume was observed between control (2356 ± 746) and all of the treatment groups ($*P<0.05$, $**P<0.01$; Figure 5b). As compared with mock, treatment with NV1023 (1575 ± 552), NV1042 (1087 ± 254) and VB (1623 ± 611) resulted in a notable reduction in tumor size, whereas the combination of NV1023/VB (1143 ± 321) was superior to either therapy alone. Importantly, NV1042 plus VB (487 + 175, $***P<0.01$) was significantly more effective than NV1023 plus VB or NV1042 alone. These combination therapies appeared to be nontoxic to mice, as their body weight were not statistically different (Supplementary Figure 4). As the combination of NV1042/VB appeared to be more efficacious than any of the other treatment groups in reducing tumor volume, we hypothesized that this might be due, in part, to the combined antiangiogenic contributions of IL-12 and VB. This was tested using anti-CD31 antibody staining, which marks endothelial cells, on CWR22 tumor tissue sections. This revealed a reduction in $CD31^+$ cells in the NV1042 plus VB treatment group as compared with the other treatment groups (Figure 5c). A statistically significant reduction in the number of $CD31^+$ cells was observed in tumors treated with NV1042 plus VB as compared with all of the other treatment groups ($**P<0.05$; Figure 5d). In addition, statistically significant differences were also observed between NV1023 and NV1042 treatment groups ($*P<0.05$), which is consistent with a previous report demonstrating a reduction of CD31-positive cells in murine prostate tumors treated with NV1042.[8]

Lastly, we wished to confirm specificity in an additional model system representative of human prostate cancer. Recently, we reported the use of human prostate organ cultures using surgical specimens derived from radical prostatectomies to assess oHSV target specificity and replication competence.[23] We exploited this

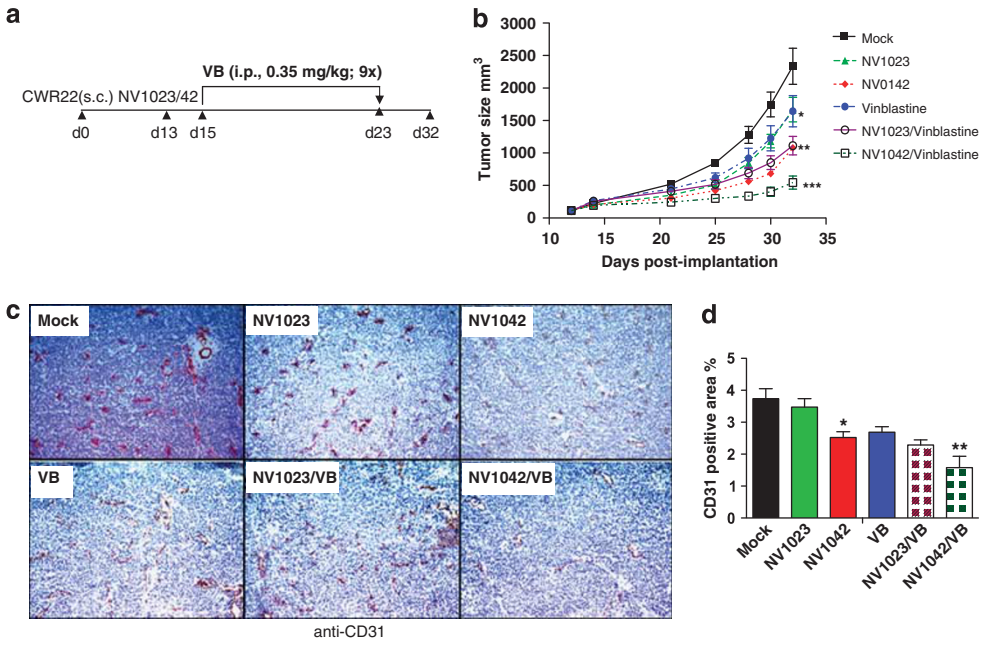

Figure 5. *In vivo* efficacy studies. (**a**) Schematic illustrating the dosing and scheduling of single and combination treatment regimes in mice bearing subcutaneous CWR22 tumors. (**b**) Assessment of CWR22 tumor growth. Virus (NV1023 or NV1042; 5×10^5 plaque-forming units (pfu)) or virus suspension buffer (phosphate-buffered saline with 10% glycerol) was injected intratumorally on days 13 and 15 after tumor implantation. Vinblastine (VB) was administered intraperitoneally at 0.35 mg kg^{-1} on day 15 for 9 consecutive days. *$P<0.05$ for mock ($n=8$) versus NV1023 only ($n=8$) and VB only ($n=7$); **$P<0.01$ for mock versus NV1042 only ($n=6$) and NV1023 + VB ($n=6$); ***$P<0.01$ for NV1042 + VB ($n=7$) versus NV1042 only and NV1023 + VB at day 32. (**c**) Evaluation of CD31$^+$ staining (brown) as a function of treatment condition. Mice ($n=3$ per group) were treated as described above, and at day 30 post-implantation tumors were collected, frozen and cut into tissue sections. Tissue sections were stained with a rat anti-mouse CD31 antibody and were counterstained with hematoxylin. (**d**) Quantification of CD31-positive staining. Tumor microvessel density was quantified for all treatment groups. Tumor microvessel density was compared between all treatment groups and untreated control group. (mean ± s.e.m.); *$P<0.04$ for NV1023 versus NV1042; **$P<0.03$ for NV1042 versus NV1042/VB.

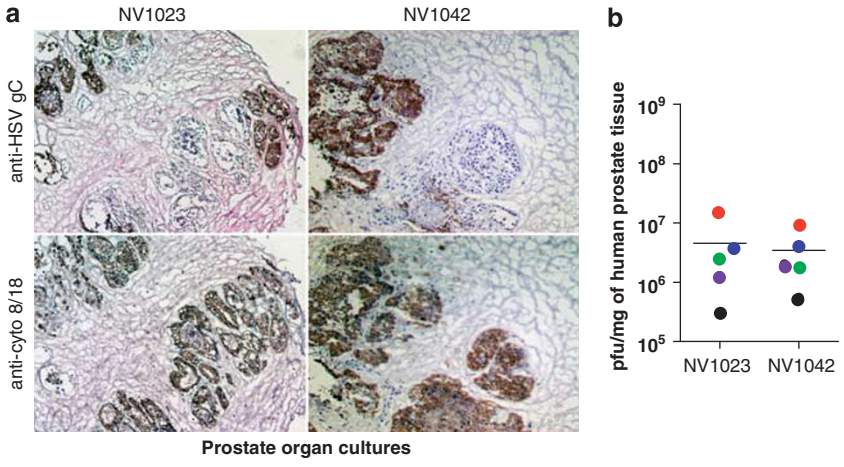

Figure 6. Analysis of NV1023 and NV1042 infection of prostate cancer surgical samples. Tissues were incubated with NV1023 (1×10^6 plaque-forming units (pfu)) or NV1042 (1×10^6 pfu) for 1 h in direct contact and, thereafter, placed on a semi-submersed collagen sponge for 3 days. (**a**) Tissue specimens were stained with anti-herpes simplex virus-1 (HSV-1) gC (upper panels) or anti-cytokeratin-8/18 (lower panels) antibodies. Sections were counterstained with hematoxylin. Note the partial overlap between anti-HSV gC and cytokeratin-8/18$^+$ staining. (**b**) Evaluation of NV1023 or NV1042 replication in prostate organ cultures. Each color dot indicates a different prostate surgical specimen. Horizonal line denotes the average viral titer for the two groups, which are statistically not significant. Note that infection with NV1023 or NV1042 resulted in similar viral titers. The five specimens examined represent Gleason Scores of either 3 + 3 = 6 or 3 + 4 = 7.

system to address the target specificity and replication competence of NV1023 and NV1042. At 3 days after infection, anti-HSV gC staining revealed that both NV1023 and NV1042 appeared to preferentially localize to the prostatic glandular regions in primary human prostate cancer tissues (Figure 6a). The staining of serial sections with anti-cytokeratin-8/18 antibody, which specifically stains luminal epithelial cells, confirmed that both vectors were restricted to epithelial cells and is in agreement with the restricted specificity of oHSVs previously seen in prostate cancer tissues.[23] NV1023 and NV1042 replicated to similar degrees in five different prostate cancer tissue specimens examined (Figure 6b). Interestingly, the amount of replication for both viruses was similar in cultures from the same patient (same color dots, Figure 6b) as opposed to different patients.

DISCUSSION

The discovery that tumors induce angiogenesis to generate new blood vessels for their growth and progression[25,26] has recently led to numerous antiangiogenic therapeutic strategies as well as demonstrated promise in improving the outcomes in cancer patients.[27] Our study focused on implementing a treatment regimen for prostate cancer by combining the antitumor and antiangiogenic activities of an 'armed' oHSV (NV1042) with a cytotoxic MDA, VB, to improve antitumor efficacy. Of the six MDAs tested, we found VB to be the most potent at killing not only prostate cancer cells but also all endothelial cells. This is in agreement with published observations that show that continuous treatment of VB at a low dose can result in antiangiogenesis and sustained tumor regression.[28]

Strategies of 'arming' oHSVs with antiangiogenic transgenes have also shown promise in various preclinical models. For instance, IL-12-expressing NV1042 has shown enhanced therapeutic efficacy over NV1023 in subcutaneous or metastatic lung murine prostate cancer TRAMP-C2 tumors[9,10] and C3(1)/T-Ag breast cancers.[29] In addition, 'armed' oHSVs expressing other antiangiogenic agents such as dominant-negative fibroblast growth factor receptor, platelet factor-4 or angiostatin have been shown to substantially decrease blood vessel formation and increase survival.[30–32]

In vivo, we demonstrate that the combination of IL-12-expressing NV1042 with low-dose VB can enhance CWR22 tumor killing by partially impairing endothelial cell growth and/or neovascularization. VB alone administered at a low dose ($0.35\,mg\,kg^{-1}$) over a 9-day period or NV1042 monotherapies were effective at promoting tumor regression. However, in combination a superior antitumor effect was observed, accompanied by minimal adverse side effects, such as stable body weight. The decreased tumor growth elicited by combining NV1042 with VB was most likely due to the cooperative effect on blood vessels as shown by the significant decrease in CD31+ blood vessels as well as the cytotoxic effects on tumor cells by either agent. Angiogenesis is a complex process that involves multiple regulatory proteins and endothelial cell activation. Endothelial cells that make up existing blood vessels are activated to multiply and migrate as surrounding basement membrane, and extracellular matrix is degraded to make way for new capillaries. IL-12 primarily modulates tumor growth by the recruitment of immune cells such as natural killer cells and T cells.[33] Our previous work addressed the antitumor and antiangiogenic properties of the NV1042 expressing IL-12 virus in both syngeneic and transgenic mouse models of prostate cancer.[8–10] In this paper, our study focused on the antiangiogenic effects of NV1042 in combination with VB in human prostate cancers. Therefore, we utilized athymic xenograft models of prostate cancer, which lack T cells and, therefore, eliminates the tumor regression effects contributed by T cells.[34] However, nude and severe-combined immunodeficient mice have relatively normal levels of natural killer cells, which have been shown to contribute, in part, to the inhibition of angiogenesis by IL-12.[11,35] Our data show that NV1042 was superior to NV1023 either alone or in combination with VB in slowing tumor growth in nude mice and that these results correlated with the percentage CD31+ blood vessels in tumor xenografts as a function of treatment condition.

Previous studies have shown that chemotherapy can enhance oncolytic viral replication.[36] *In vitro*, we did not observe any significant change in NV1042/NV1023 viral yield in the presence of VB. This is in accordance with our previous findings, in which pretreatment with nontoxic concentrations of taxanes had negligible effects on G47Δ replication.[13] A similar dose range of either docetaxel or paclitaxel in combination with G47Δ significantly increased prostate cancer cell killing.[13] In the present study, irrespective of treatment sequence with the combination of NV1023/NV1042 and VB, a weak synergy-to-additive effect was observed. As α-herpes viruses are dependent on intact microtubules for efficient transport and egress,[37] MDA treatment would be expected to compromise NV1023/N1042 replication, particularly under conditions where VB was added before virus infection. Disruption of microtubules by MDAs, such as nocodazole or taxol (that is, paclitaxel), have shown varying effects on HSV-1 transport and replication. Avitabile *et al.*[38] reported that neither MDA significantly affected the release of free virus into the media at micromolar concentrations. In contrast, Kotaskis *et al.*[39] reported that treatment of synchronized cells with nocadozale or taxol at similar concentrations prevented optimal HSV-1 replication. These discrepancies may be attributed to whether cells were synchronized or, alternatively, due to differences in the sensitivities of cells to nocodazole or taxol. A likely explanation for the observed weak synergy-to-additive effects is that at low VB concentrations, microtubules are minimally disrupted, which would allow for sufficient NV1023/NV1042 replication. In agreement with these observations, the addition of G207 to nanomolar concentrations of paclitaxel resulted in weak synergy in promoting thyroid cancer cell killing with minimal effects on G207 replication.[40]

Combination therapy regimens with antiangiogenic agents will be critical to treat prostate cancer, as microvessel density has been shown to correlate strongly with Gleason grade and predict disease progression.[41,42] Although a recently concluded phase III trial of prostate cancer using bevacizumab (anti-vascular endothelial growth factor antibody) in addition to the current standard of docetaxel and prednisone was negative,[43] other antiangiogenic strategies are worth exploring, and the use of dual angiogenesis inhibition with direct oncolytic oHSV therapy is an attractive strategy for prostate cancer and can hopefully be used to overcome resistance that is observed with antiangiogenic monotherapies.[44]

CONFLICT OF INTEREST

The authors declare no conflict of interest.

ACKNOWLEDGEMENTS

This study was supported in part by a grant to RLM (R01CA102139). We thank Melissa Marinelli for laboratory assistance. We also thank Dr K Pienta (University of Michigan) for the bone marrow-derived HBME-1 endothelial cells.

REFERENCES

1 Martuza RL, Malick A, Markert JM, Ruffner KL, Coen DM. Experimental therapy of human glioma by means of a genetically engineered virus mutant. *Science* 1991; **252**: 854–856.
2 Mineta T, Rabkin SD, Yazaki T, Hunter WD, Martuza RL. Attenuated multi-mutated herpes simplex virus-1 for the treatment of malignant gliomas. *Nat Med* 1995; **1**: 939–943.
3 Varghese S, Rabkin SD. Oncolytic herpes simplex virus vectors for cancer virotherapy. *Cancer Gene Ther* 2002; **9**: 967–978.
4 Kuruppu D, Tanabe KK. Viral oncolysis by herpes simplex virus and other viruses. *Cancer Biol Ther* 2005; **4**: 524–531.
5 Kaur B, Chiocca EA, Cripe TP. Oncolytic HSV-1 virotherapy: clinical experience and opportunities for progress. *Curr Pharm Biotechnol* 2012; **13**: 1842–1851.
6 Wong RJ, Patel SG, Kim S, DeMatteo RP, Malhotra S, Bennett JJ *et al.* Cytokine gene transfer enhances herpes oncolytic therapy in murine squamous cell carcinoma. *Hum Gene Ther* 2001; **12**: 253–265.
7 Wong RJ, Chan MK, Yu Z, Ghossein RA, Ngai I, Adusumilli PS *et al.* Angiogenesis inhibition by an oncolytic herpes virus expressing interleukin 12. *Clin Cancer Res* 2004; **10**: 4509–4516.
8 Varghese S, Rabkin SD, Liu R, Nielsen PG, Ipe T, Martuza RL. Enhanced therapeutic efficacy of IL-12, but not GM-CSF expressing oncolytic herpes simplex virus for transgenic mouse derived prostate cancers. *Cancer Gene Ther* 2005; **13**: 253–265.

9 Varghese S, Rabkin SD, Nielsen PG, Wang W, Martuza RL. Systemic oncolytic herpes virus therapy of poorly immunogenic prostate cancer metastatic to lung. *Clin Cancer Res* 2006; **12**: 2919–2927.
10 Varghese S, Rabkin SD, Nielsen GP, MacGarvey U, Liu R, Martuza RL. Systemic therapy of spontaneous prostate cancer in transgenic mice with oncolytic herpes simplex viruses. *Cancer Res* 2007; **67**: 9371–9379.
11 Duda DG, Sunamura M, Lozonschi L, Kodama T, Egawa S, Matsumoto G *et al.* Direct *in vitro* evidence and *in vivo* analysis of the antiangiogenesis effects of interleukin 12. *Cancer Res* 2000; **60**: 1111–1116.
12 Mitola S, Strasly M, Prato M, Ghia P, Bussolino F. IL-12 regulates an endothelial cell-lymphocyte network: effect on metalloproteinase-9 production. *J Immunol* 2003; **171**: 3725–3733.
13 Passer BJ, Castelo-Branco P, Buhrman JS, Varghese S, Rabkin SD, Martuza RL. Oncolytic herpes simplex virus vectors and taxanes synergize to promote killing of prostate cancer cells. *Cancer Gene Ther* 2009; **7**: 551–560.
14 Lin SF, Gao SP, Price DL, Li S, Chou TC, Singh P *et al.* Synergy of a herpesoncolytic virus and paclitaxel for anaplastic thyroid cancer. *Clin Cancer Res* 2008; **14**: 1519–1528.
15 Huang B, Sikorski R, Kirn DH, Thorne SH. Synergistic anti-tumor effects between oncolyticvaccinia virus and paclitaxel are mediated by the IFN response and HMGB1. *Gene Ther* 2011; **18**: 164–172.
16 Heinemann L, Simpson GR, Boxall A, Kottke T, Relph KL, Vile R *et al.* Synergistic effects of oncolyticreovirus and docetaxel chemotherapy in prostate cancer. *BMC Cancer* 2011; **11**: 221.
17 Radhakrishnan S, Miranda E, Ekblad M, Holford A, Pizarro MT, Lemoine NR *et al.* Efficacy of oncolytic mutants targeting pRb and p53 pathways is synergistically enhanced when combined with cytotoxic drugs in prostate cancer cells and tumor xenografts. *Hum Gene Ther* 2010; **10**: 1311–1325.
18 Oberg D, Yanover E, Adam V, Sweeney K, Costas C, Lemoine NR *et al.* Improved potency and selectivity of an oncolytic E1ACR2 and E1B19K deleted adenoviral mutant in prostate and pancreatic cancers. *Clin Cancer Res* 2010; **16**: 541–553.
19 Schwartz EL. Antivascular actions of microtubule-binding drugs. *Clin Cancer Res* 2009; **15**: 2594–2601.
20 Wong RJ, Patel SG, Kim S, DeMatteo RP, Malhotra S, Bennett JJ *et al.* Cytokine gene transfer enhances herpes oncolytic therapy in murine squamous cell carcinoma. *Hum Gene Ther* 2001; **12**: 253–265.
21 Meignier B, Longnecker R, Roizman B. *In vivo* behavior of genetically engineered herpes simplex viruses R7017 and R7020: construction and evaluation in rodents. *J Infect Dis* 1988; **158**: 602–614.
22 Chou TC, Talalay P. Quantitative analysis of dose-effect relationships: the combined effects of multiple drugs or enzyme inhibitors. *Adv Enzyme Regul* 1984; **22**: 27–55.
23 Passer BJ, Wu C-L, Wu S, Rabkin SD, Martuza RL. Analysis of genetically engineered oncolytic herpes simplex viruses in human prostate cancer organotypic cultures. *Gene Ther* 2009; **16**: 1477–1482.
24 Kanthou C, Tozer GM. Tumour targeting by microtubule-depolymerizing vascular disrupting agents. *Expert Opin Ther Targets* 2007; **11**: 1443–1457.
25 Folkman J. Anti-angiogenesis: new concept for therapy of solid tumors. *Ann Surg* 1972; **175**: 409–416.
26 Hanahan D, Weinberg RA. Hallmarks of cancer: the next generation. *Cell* 2011; **144**: 646–674.
27 Folkman J. Angiogenesis: an organizing principle for drug discovery? *Nat Rev Drug Discov* 2007; **6**: 273–286.
28 Klement G, Baruchel S, Rak J, Man S, Clark K, Hicklin DJ *et al.* Continuous low-dose therapy with vinblastine and VEGF receptor-2 antibody induces sustained tumor regression without overt toxicity. *J Clin Invest* 2000; **105**: R15–R24.
29 Liu R, Varghese S, Rabkin SD. Oncolytic herpes simplex virus vector therapy of breast cancer in C3(1)/SV40 T-antigen transgenic mice. *Cancer Res* 2005; **65**: 1532–1540.
30 Liu TC, Zhang T, Fukuhara H, Kuroda T, Todo T, Canron X *et al.* Dominant-negative fibroblast growth factor receptor expression enhances antitumoral potency of oncolytic herpes simplex virus in neural tumors. *Clin Cancer Res* 2006; **12**: 6791–6799.
31 Liu TC, Zhang T, Fukuhara H, Kuroda T, Todo T, Martuza RL *et al.* Oncolytic HSV armed with platelet factor 4, an antiangiogenic agent, shows enhanced efficacy. *Mol Ther* 2006; **14**: 789–797.
32 Zhang W, Fulci G, Buhrman JS, Stemmer-Rachamimov AO, Chen JW, Wojtkiewicz GR *et al.* Bevacizumab with angiostatin-armed oHSV increases antiangiogenesis and decreases bevacizumab-induced invasion in U87 glioma. *Mol Ther* 2012; **1**: 37–45.
33 Colombo MP, Trinchieri G. Interleukin-12 in anti-tumor immunity and immunotherapy. *Cytokine Growth Factor Rev* 2002; **13**: 155–168.
34 Voest EE, Kenyon BM, O'Reilly MS, Truitt G, D'amato RJ, Folkman J. Inhibition of angiogenesis *in vivo* by interleukin 12. *JNCI* 1995; **87**: 581–586.
35 Yao L, Sgadari C, Furuke K, Bloom ET, Teruya-Feldstein J, Tosato G. Contribution of natural killer cells to inhibition of angiogenesis by interleukin-12. *Blood* 1999; **5**: 1612–1621.
36 Yu DC, Chen Y, Dilley J, Li Y, Embry M, Zhang H *et al.* Antitumor synergy of CV787, a prostate cancer-specific adenovirus, and paclitaxel and docetaxel. *Cancer Res* 2001; **61**: 517–525.
37 Penfold MET, Armati P, Cunningham AL. Axonal transport of herpes simplex virions to epidermal cells: Evidence for a specialized mode of virus transport and assembly. *Proc Natl Acad Sci USA* **91**: 6529–6533.
38 Avitabile E, Di Gaeta S, Torrisi MA, Ward PL, Roizman B, Campadelli-Fiume G. Redistribution of microtubles and golgi apparatus in herpes simplex virus-infected cells and their role in viral exocytosis. *J Virol* 1995; **69**: 7472–7782.
39 Kotaskis A, Pomeranz LE, Blouin A, Blaho JA. Microtubule reorganization during herpes simplex virus type I infection facilitates nuclear localization of VP22, a major virion tegment protein. *J Virol* 2001; **75**: 8697–8711.
40 Lin S-F, Gao SP, Price DL, Li S, Chou T-C, Singh P *et al.* Synergy of a herpes oncolytic virus and paclitaxel for anaplastic thyroid cancer. *Clin Cancer Res* 2008; **14**: 1519–1528.
41 Weidner N, Carroll PR, Flax J, Blumenfeld W, Folkman J. Tumor angiogenesis correlates with metastasis in invasive prostate carcinoma. *Am J Pathol* 1993; **143**: 401–409.
42 Gettman MT, Pacelli A, Slezak J, Bergstralh EJ, Blute M, Zincke H *et al.* Role of microvessel density in predicting recurrence in pathologic stage T3 prostatic adenocarcinoma. *Urology* 1999; **54**: 479–485.
43 Kelly WK, Halabi S, Carducci M, George D, Mahoney JF, Stadler WM *et al.* Randomized, double-blind, placebo-controlled phaseIII trial comparing docetaxel and prednisone with or without bevacizumab in men with metastatic castration-resistant prostate cancer: CALGB 90401. *J Clin Oncol* 2012; **30**: 1534–1540.
44 Kerbel RS, Yu J, Tran J, Man S, Viloria-Petit A, Klement G *et al.* Possible mechanisms of acquired resistance to anti-angiogenic drugs: implications for the use of combination therapy approaches. *Cancer Metastasis Rev* 2001; **20**: 79–86.

Supplementary Information accompanies the paper on Cancer Gene Therapy website (http://www.nature.com/cgt)